220 GHZ ZENITH ATMOSPHERIC TRANSPARENCY AT IAO, HANLE *

P.G. Ananthasubramanian[1], Satoshi Yamamoto[2], and Tushar P. Prabhu[3]
[1]Raman Research Institute, Bangalore 560 080, India
[2]Dept. of Physics, University of Tokyo, Bunkyo-ku, Tokyo 113, Japan
[3]Indian Institute of Astrophysics, Bangalore 560 034, India.

Abstract

We present 220 GHz (1.36 mm) measurements of zenith optical depth obtained to characterise the Indian Astronomical Observatory, Hanle (Ladakh, India) during the period from late December 1999 to early May 2000 and early October 2000 to September 2001. The data were sampled at an interval of 10 minutes. We describe the automated 220 GHz tipping radiometer used, its basic principle, operation, data acquisition method and data reduction scheme in detail. The 220 GHz opacity is found to be less than 0.06 for a significant fraction (40%) of the time during the winter months, indicating that Hanle is one of the good observing sites for submillimeter-wave astronomy. We make a preliminary correlation with the precipitable water vapour derived from surface relative humidity and air temperature measurements made during the same period with a weather station installed at the site. We also compare the Hanle site with other high-altitude sites like Mauna Kea and Atacama desert.

keywords: atmospheric opacity, precipitable water vapour (pwv), surface water vapour pressure(P_o), superheterodyne receiver, sub-mm astronomy and mm-wave astronomy

* Hanle : Latitude 32°46′46″ N; Longitude 78°57′51″ E; Altitude 4500 m

Introduction

Until recently, the only well-established high-altitude astronomical site in the northern hemisphere was Mauna Kea, Hawaii (altitude 4100 m). Mt Evans (4300 m) in Colorado is currently being developed by the University of Denver. The Indian Astronomical Observatory (IAO) was set up recently in the high-altitude cold desert of Changthang ("highlands") Ladakh [1] with a 2-m aperture optical-infrared telescope [2, 3]. IAO is atop Mt. Saraswati (4500 m), Digpa-ratsa Ri, a range of hillocks surrounded by vast plains (Nilamkhul Plain at 4300 m).

The electromagnetic spectrum in the sub-mm region is not so well explored for astronomy as yet. Apart from the JCMT and CSO at Mauna Kea in the northern hemisphere, there are only a few other facilities setup for observations in this wavelength band, e.g. Gornergrat, in Switzerland (altitude 3167 m) and Mt. Fuji in Japan (3776 m). A high altitude site (4000–5000 m) has been identified in Chile for upcoming projects such as the Atacama Large Millimeter Array (ALMA). This is a well characterised site in the southern hemisphere apart from the South Pole, Antarctica (2835 m). There are other high-altitude sites proposed for mm-wave astronomy, such as Cerro La Negra (4600 m) in Mexico. The need for a high-altitude site arises primarily because atmospheric constituents like water vapour, oxygen and a few other molecules absorb a substantial portion of the incoming radiation in the sub-mm spectral region and such absorption reduces as one goes to higher altitudes. The atmosphere not only reduces the signal strength but also contributes to an increase in system temperature and thus doubly degrades the system sensitivity. Of the various atmospheric constituents, oxygen content is fairly constant both diurnally and seasonally for a given location, and depends on its latitude and altitude. The water vapour content, on the other hand, varies both diurnally and seasonally. There are some semitransparent windows between the emission/absorption bands, which lie in the troughs formed between the wings of the bands. The trasmission in these wings improves with altitude.

There are several emission lines and bands of astrophysical interest in the available windows: 346 GHz (CO $J = 3$–2), 460 GHZ (CO J=4–3), 492 GHz (C I), 660 GHz (^{13}CO J=6–5), 692 GHz (CO J=6–5), 806 GHz (CO J=7–6) and 880 GHz (^{13}CO J=8–7). Ideally, it will be important to monitor any prospective site for its atmospheric transmission quality in these windows before a large investment is made for a major facility. Since sub-mm instrumentation is very expensive and requires considerable logistic support, it has been a general practice to monitor the atmospheric transmission at lower frequencies such

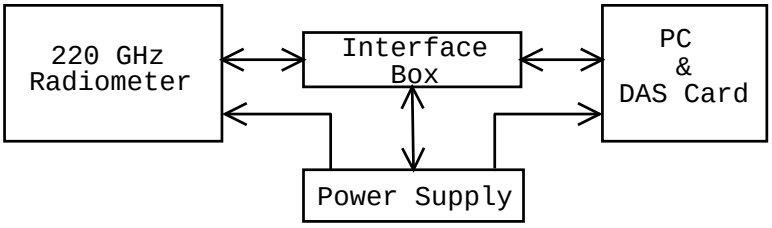

Figure 1. A block diagram of the radiometer system showing all the four different units. Only the 220 GHz radiometer is installed outdoors on a pedestal at about 3 m above the ground. The other three units are housed inside the seeing monitor building located near the pedestal (see Fig. 3).

as 183, 220 or 225 GHz in the mm-wave region. The transparencies in the higher frequency windows can be scaled using suitable models of earth's atmosphere. Some of these measurements are discussed by [4, 5, 6, 7, 8, 9, 10].

The identification and development of the Hanle site amidst a vast cold desert landscape, where the ambient temperatures go down to -25° C during winter nights, opens up possibilities for setting up of future large observing facilities in the sub-mm and lower wavelength bands in the northern hemisphere. The atmospheric transparency at the sub-mm frequencies are expected to be very good judging from the surface relative humidity and air temperature data that are being recorded at Hanle since the summer of 1996. However, it is indispensable to measure the atmospheric opacity directly at the mm-wave frequency in order to characterize the actual observing conditions at the site. Such opacity measurements have been reported for other high altitude sites, and we can compare the results of Hanle with these quantitatively. With this in mind, a team of Japanese astrophysicists visited the site and measured the atmospheric opacity at 220 GHz in November 1996 . At that time, the 220 GHz opacity was around 0.05, indicating good transparency even at sub-mm frequencies. Encouraged by this experiment, it was decided to operate the 220 GHz radiometer continuously at the site for a 2-year period. In this paper, we describe the first long-term results of the 220 GHz opacity measurements at IAO, Hanle.

Description of the 220 GHz system

The radiometer is essentially the same unit as used at Mt. Fuji during 1994–95 [10]. The system consists of four distinct units: (i) a 220 GHz

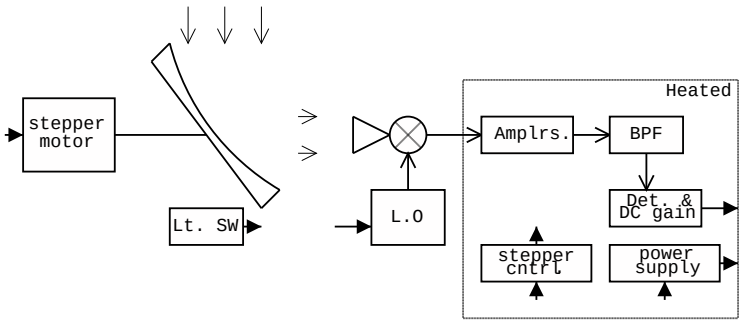

Figure 2. A schematic diagram showing some of the mm-wave and other electronics housed in the radome. The mirror scans the sky in elevation through a layer of protective membrane fixed to the rectangular window on the radome.

receiver with a stepper-motor-driven off-axis paraboloid to scan in elevation, (ii) a power supply, (iii) an interface unit and (iv) a personal computer running on DOS with a hard disk for data storage (Fig. 1). The PC communicates with both these units through an add-on card. The unit (i) is meant for outdoor use with a metal radome top of semi-cylindrical shape. The radome has a rectangular window covered with a layer of low-loss woven teflon membrane which is transparent to mm-waves. This ensures continuous safe operation of the electronics in the outdoor environment. The inner surface of the radome is packed with 50 mm thick thermal insulating material to provide some isolation from the outside sub-zero ambient temperatures. Heating of the radome was not considered necessary since snowfall is rare and negligible at the site. The small amount of wet snow in autumn and spring melts away in the subsequent sunlight and the dry snow in deep winter is blown away by the wind. The box containing the intermediate frequency (IF) electronics and the detector housed inside the radome unit is heated and maintained at 7° C (T_{heater}). The program maintains the IF box temperature by on-off control during the time between the 10 minute sky scans, should the temperature fall below this (Fig. 2).

The off-axis parabolic mirror of focal length 150 mm, with a projected aperture of 80 mm, is mounted at 45° to the rotation axis, and the 220 GHz prime-focus receiver is fixed on the rotation axis. The rotation axis is horizontal. The reflected and focussed beam is normal to the incoming radiation and lies along the rotation axis of the mirror and stepper motor as the mirror scans the sky from one horizon through the zenith to nearly the opposite horizon. With this simple arrangement,

the system can look at the sky at all elevations or zenith angles (z) at a fixed azimuth position, with just one axis rotation and no blockage. The effective beam size on the sky is about 1°.

The 220 GHz receiver is a super-heterodyne receiver consisting of a corrugated conical horn, a sub-harmonically pumped Schottky diode mixer and a Gunn diode local oscillator (LO) working at 110 GHz. The down-converted signal centred at 1450 MHz is amplified by a low-noise amplifier and a post-amplifier, and passed through a band-pass filter (BPF) to limit the bandwidth to 500 MHz. The band-limited signal is square-law detected and amplified for digitising. Digitising is done by a commercial PC add-on analog-to-digital converter and digital input/output card which is also used for controlling the stepper motor movement. There is no encoder to identify the beam position on the sky. A sky scan starts from a home position (zenith angle about$-90°$) identified with a limit-switch status. A typical scan starts from the home position and ends at the home position, passing through the zenith position. The program also monitors system power supply voltages and temperatures inside the radome and on the IF box (Fig. 2).

The mirror with a beam size about 1° on sky is driven by a stepper motor under PC control. It is programmed to look at every 0.72° in zenith angle on the sky for 90 ms, covering a zenith angle range of nearly $-90°$ to $+70°$. The sky coverage through the radome window is limited to about 90°, i.e., from about $-75°$ to $+15°$ in zenith angle. A forward scan and a reverse scan are taken in about 50 s. Between $+22°$ and $+60°$ zenith angle position is a reference load, a blackbody at room temperature (T_{ref}). The averaged signal corresponding to these mirror positions is the reference for temperature calibration of the signal received from the sky emission. Data are recorded with time stamp along with the monitored parameters as well as the fitted opacity values. A separate file is also generated, one for a day, wherein the time stamp, raw data file name, fitted opacity and some monitored system parameter values are recorded for every pair of scans. The program is configured to take about 144 scans in 24 hours, i.e., a pair of scans every 10 minutes.

The instrument was installed on a pedestal at about 3 m above the ground level, close to a seeing monitor and an automated weather station (Fig. 3). The radiometer power supply, interface unit and the control computer are located inside the building that houses the seeing monitor. The system was switched on for continuous measurements of the zenith optical depth on 23 December 1999.

Till May 2000, the system was in effect sampling the western sky as it was oriented to take scans in the west to east direction. After that, it was re-oriented to sample the northern sky with the scans being

Figure 3. A view of the 220 GHz radiometer on the pedestal by the side of the seeing monitor building. Also seen is the weather station.

taken in the north to south direction. This change was carried out to eliminate direct heating of components inside the radome by the Sun at low elevations and a suitable cover was fixed to provided shade in order to reduce heating by the Sun at high elevations in the new orientation.

System sensitivity

The system sensitivity expressed as the minimum detectable signal power (1σ) is given by the following expression.

$$T_{\rm rms} = T_{\rm sys}/[BW \times \text{Integration time}]^{1/2} \qquad (1)$$

In this case, the system temperature and receiver temperature are about the same i.e., $T_{\rm sys} = T_{\rm rx}$ as $T_{\rm rx} = 13,000$ K.

BW is pre-detection bandwidth = 500×10^6 Hz
Integration time = 90×10^{-3} s
System sensitivity or minimum detectable signal power T_{rms} is 2 K.

Sky scans and Analysis

The signal received from the sky (Fig. 4) suffers reduction in amplitude due to absorption and there is an additive noise contribution as well. The basic equations relating the detected voltage and temperature are:

$$V_{\rm sky} = C[T_{\rm rx} + T_{\rm sky}] \quad (2)$$

$$V_{\rm ref} = C[T_{\rm rx} + T_{\rm ref}] \quad (3)$$

where, $T_{\rm sky} = T_{\rm medium}(1 - e^{-\tau_o \sec(z)}) + T_b e^{-\tau_o \sec(z)}$, C is a proportionality constant or conversion factor, $T_{\rm rx}$ is receiver noise temperature and T_b is background source temperature which is of the order of a few Kelvin. With the assumptions that the system gain is constant or any variation is corrected, system sensitivity is the same at all zenith angles, sky is stable during the scans, no background source in the beam and $T_{\rm medium} = T_{\rm ambient} = T_{\rm ref}$, the above equations can be reduced to a single linear equation and the zenith optical depth can be determined by a least square fit routine using the $\sec(z)$ dependency of the sky emission. Data up to an airmass of about 2.5 are used in the fit to derive the zenith opacity. Data from a higher airmass may contain noise picked up from the ground and will also introduce large errors in the fitted zenith optical depth due to uncertainties in identifying the actual zenith position.

If the IF box temperature ($T_{\rm heater}$) is below 10° C, then the scans are taken with the gain increasing linearly. Otherwise, the gain variations are very slow and proportional to the slow diurnal variations of ambient temperature. Averaging the forward and reverse scans reduces the errors on the deduced optical depth due to small gain variations between the scans, and if the gain change is linear with time then averaging completely cancels the gain variations.

Results and Interpretation

The opacity values between 23 December 1999 and 12 May 2000 have larger errors due to imperfect gain cancellation between the forward and reverse scan pairs in a 10 minute sample. About 10% of the data during this period were rejected being totally unusable. The system was

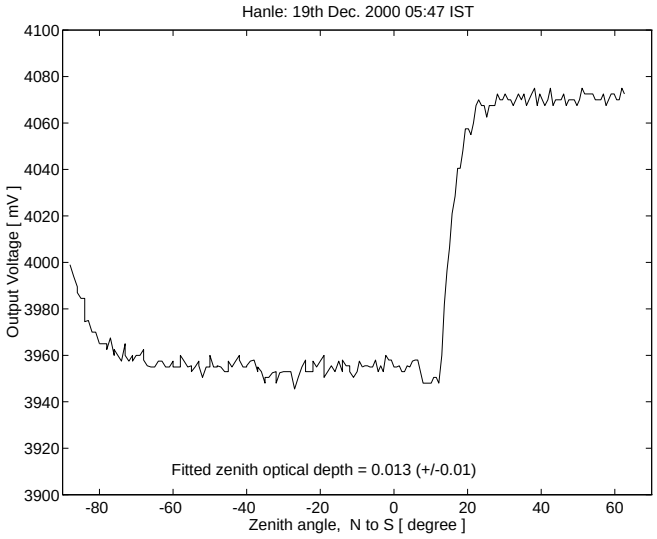

Figure 4. A typical averaged scan, detected voltage as a function of zenith angle. The trace from zenith angle between 15° and 22° is the transition voltage as the mirror begins to partially look at sky and the absorber. The higher voltage between 22° and 60° is the reference voltage when the mirror fully looks at the absorber.

also unstable, working intermittently from April to August, and fully stopped functioning by September 2000. The troubleshooting and rectification of bugs and also the overhauling and improvements undertaken in October 2000 have made the system reliable since then. The best month during the period subsequent to October 2000 was December and the observed opacities for this month are shown in Fig. 5, where the opacities are averaged over hourly intervals (7 scans including both the end points).

The 1σ error on the 220 GHz zenith optical depth from the fit is of the order of 0.01 and systematic errors are expected to be under 15%. The systamatic errors may be contributed by the following factors.

1. Error in the identification of true zenith position
2. Error due to reflections between the receiver horn and membrane resulting in a ripple in the output voltage
3. Leftover residual non-linear gain effects
4. The absorber temperature being higher than the temperature of the medium (effective atmosphere)

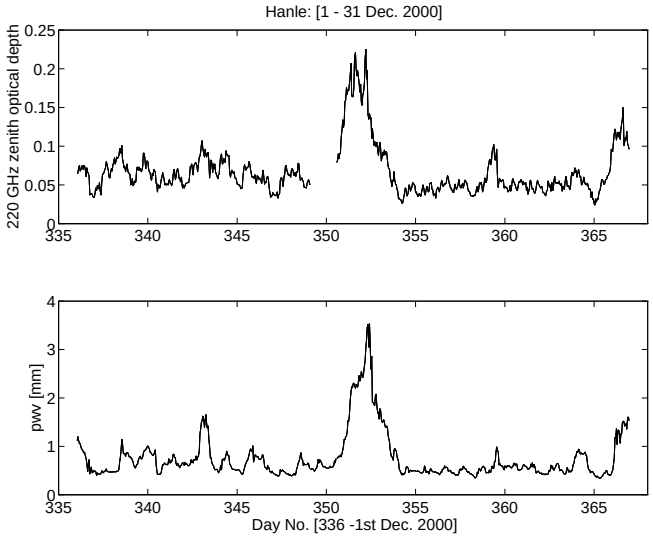

Figure 5. The derived opacities (hourly average) during the month of December 2000 (top panel). The bottom panel shows the precipitable water vapour estimated from the surface-weather-data.

The peak-to-peak errors on the determined zenith position are of the order $\pm 2.7^{\circ}$.

The fitted opacity may be negative or an overestimate if the atmosphere was non-uniform. For example the opacities will be negative if the atmosphere was to be non-uniform or with clouds near zenith and may be an overestimate if there were clouds in the beam at low elevations. We have neglected fitted opacity values that are negative, but retained all the high values though some of them may be spurious. This will lead to a slightly skewed distribution to higher opacity values, but the median of the distribution would be affected little.

An automated weather station has been installed at Hanle in July 1996 and hourly data is available on air temperature and relative humidity besides soil temperature, wind velocity vector, solar radiation and rainfall. The partial pressure of water vapour at the surface can be computed from the saturation water vapour pressure at the ambient temperature and the surface relative humidity [11, 12]:

$$P_0 = 2.409 \times 10^{12} RH (300/T)^4 e^{-6792/T} \tag{4}$$

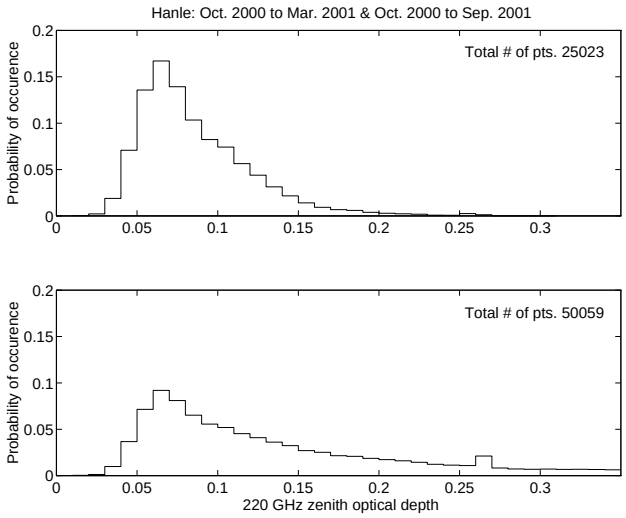

Figure 6. Relative frequency distribution of 220 GHz zenith optical depth for the period 6th October 2000 to 31st March 2001 (top panel) and 6 October 2000 to 30 September 2001 (bottom panel).

where, P_0 is the surface water vapour pressure (WVP) in microbars, RH is the relative humidity in %, and T is the surface air temperature in K.

The total water vapour content (in mm) above the surface can then be calculated using the expression below, when the surface temperature lies in the 250 to 310 K range.

$$pwv = P_0/(3.0 \times T) \tag{5}$$

where, pwv is the total precipitable water vapour column above the site in mm, and a scale height of water vapour in $H = 1.5$ km is assumed. The scale height is known to vary diurnally and seasonally, and is expected to be in the 1 to 2 km range. The lower panel of Fig. 5 shows the computed precipitable water vapour for the month of December 2000. A correlation between opacity and pwv is clearly evident.

The relative frequency distribution of zenith optical depth is shown in Fig. 6 separately for the winter months (October 2000 to March 2001), and the entire duration of observations (October 2000 to September 2001). The corresponding cumulative frequency distribution functions are shown in Fig. 7.

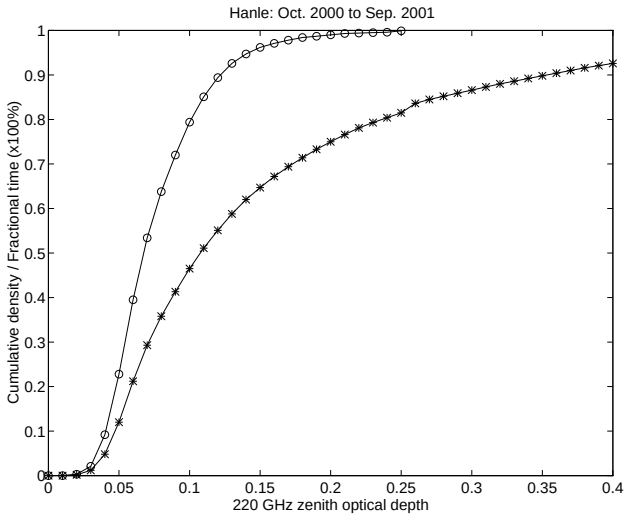

Figure 7. Cumulative density distribution function of the 220 GHz zenith optical depth. ∘ – distribution for the period 6 October 2000 to 31 March 2001 i.e., winter 2000–01. * – distribution for the period 6 October 2000 to 30 September 2001.

The 220 GHz zenith optical depth is expected to be correlated with the precipitable water vapour above the site as was brought out by Fig. 5. We proceed to derive such a relationship using the (median) quartiles of the frequency distribution of optical depth and the (median) quartiles of *pwv* derived from meteorological parameters. The plot in Fig. 8 for the period October 2000 to September 2001 with H = 1.5 km yields the following correlations:

$$\tau_{220} = 0.0281 + 0.0462 pwv \tag{6}$$

$$\tau_{220} = 0.0377 + 0.0363 pwv \ \ + 0.0014 pwv^2 \tag{7}$$

The relationship between *pwv* derived from 183 GHz water vapour line measurement (assumed H = 2 km) and the 225 GHz opacity measurements at Atacama (5000 m) is [13]

$$\tau_{225} = 0.007 + 0.041 pwv + 0.0009 pwv^2 \tag{8}$$

The opacity at 220 GHz is expected to be about 19% lower compared to the 225 GHz opacity (in the range 0.06 to 0.12). Thus, the relationship derived by us is (slightly) steeper, and has an appreciable offset. It is likely that the offset results from residual systematic errors mentioned earlier in this section. While the slopes can be affected by systematic

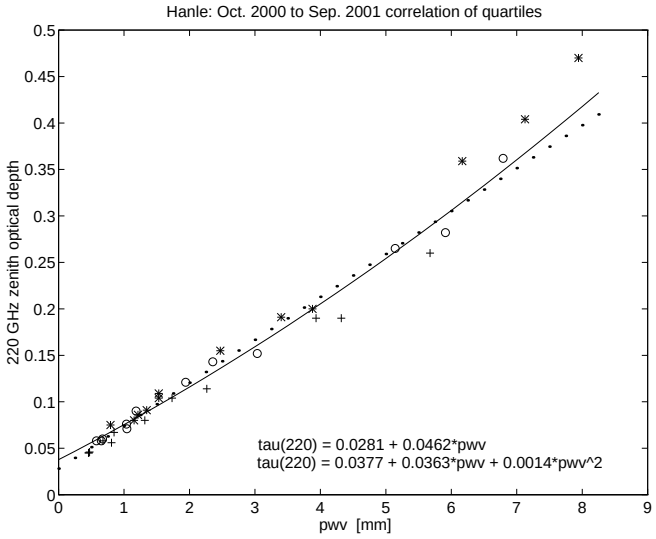

Figure 8. A plot of the quartiles of measured opacities, and the quartiles of precipitable water vapour column derived from weather parameters for an assumed scale height of 1.5 km. +: first quartile; ○: median; *: third quartile. A least square linear fit is shown as dotted line and a quadratic fit by continuous line.

percentile errors in the opacity estimates, the major source of error could also be contributed by the uncertainty in the mean scale height.

The early determinations of optical depth (1999 December – 2000 May), though having larger errors, agree with the weather derived *pwv* in their quartiles. We thus believe that the early measurements are on the average consistent with the current set of improved data. The zenith optical depth quartiles for both these periods are shown in Fig. 9, as also listed in Table 1.

The 225 GHz zenith optical depth quartiles at Mauna Kea for the nearly three year period (January 1997 – October 2000) are 0.058, 0.091, 0.153. The opacity at at 220 GHz is expected to be lower by about 19% compared to the 225 GHz opacity (in the range 0.06 to 0.12). Thus, the transparency of Hanle during October 2000 – September 2001 (one year period: 0.065, 0.108, 0.200) is slightly higher than the annual average at Mauna Kea. In Fig. 10 the one to one comparison of 225 GHz median opacities at Hanle and Mauna Kea for the period October 2000 to March 2001 indicates Hanle to be slightly better than Mauna Kea in deep winter (December – February) and comparable over the period October – March. The Mauna Kea opacities are shown in the figure

Table I. Percentile opacities at 220 GHz, IAO, Hanle

Month	Year	Q1	Q2	Q3
January	2000	0.055	0.079	0.105
	2001	0.045	0.058	0.080
February	2000	0.055	0.076	0.098
	2001	0.045	0.060	0.086
March	2000	0.059	0.082	0.110
	2001	0.058	0.076	0.104
April	2000	0.074	0.108	0.148
	2001	0.080	0.121	0.155
May	2000	0.096	0.136	0.194
	2001	0.104	0.143	0.191
June	2001	0.190	0.265	0.359
July	2001	0.260	0.362	0.470
August	2001	0.190	0.282	0.404
September	2001	0.114	0.152	0.200
October	2000	0.056	0.071	0.091
November	2000	0.067	0.090	0.109
December	1999	0.040	0.060	0.085
	2000	0.046	0.058	0.075

after conversion to equivalent 220 GHz opacities using expressions from [9].

The relation between 220 GHz opacity (τ_{220}) and the submillimeter-wave opacity has been measured at Atacama [5]:

$$\tau_{492} = 21.7 \times \tau_{220} + 0.270 \quad (9)$$

$$\tau_{675} = 20.7 \times \tau_{220} + 0.063 \quad (10)$$

where, τ_{492} and τ_{675} denote the opacities at 492 GHz and 675 GHz respectively. Therefore, the 220 GHz opacity of 0.06 corresponds to the 492 GHz opacity of 1.6, which is the actual upper limit for astronomical observations.

In Fig. 11 we notice that the fractional time for τ_{220} below 0.06 at Hanle is comparable to Mauna Kea during the six winter months and is about 40%. The fractional time for τ_{220} below 0.10 (80%) is better than at Mauna Kea (64%) for the same period. The corresponding fractional time at Mt. Fuji are about 45% and about 65% respectively,

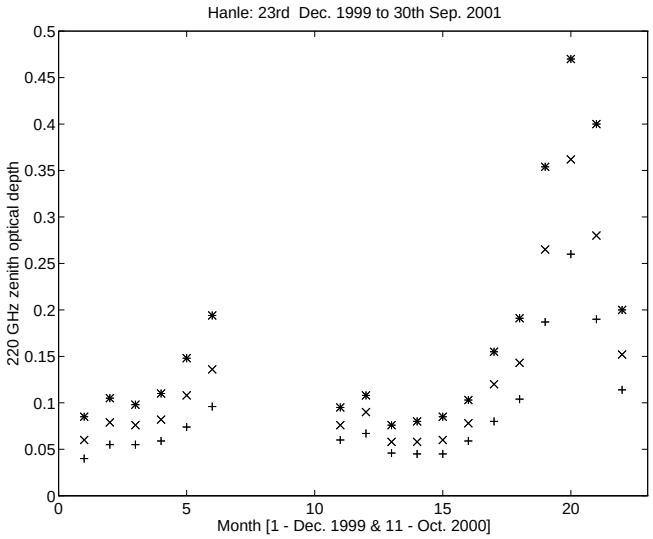

Figure 9. Monthly quartiles of 220 GHz zenith optical depth for the period 23 December 1999 to 12 May 2000 and 6 October 2000 to 30 September 2001 + – first quartile, × – second quartile (median) and * – third quartile.

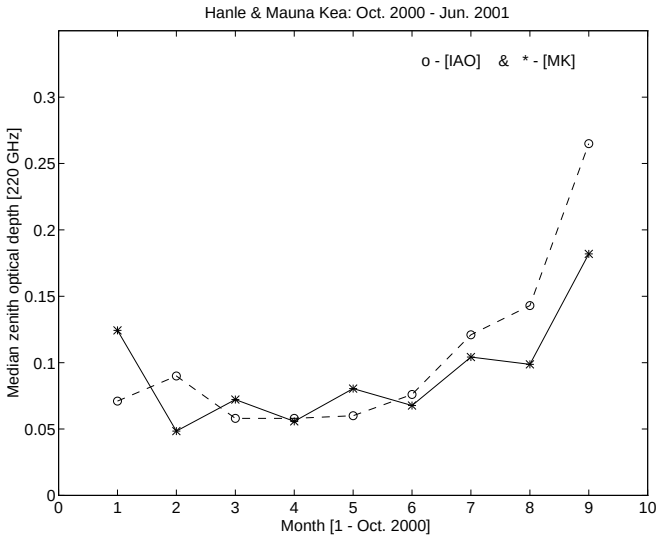

Figure 10. Monthly median opacities at IAO, Hanle and at Mauna Kea for the period October 2000 to June 2001. The Mauna Kea opacities are scaled to 220 GHz.

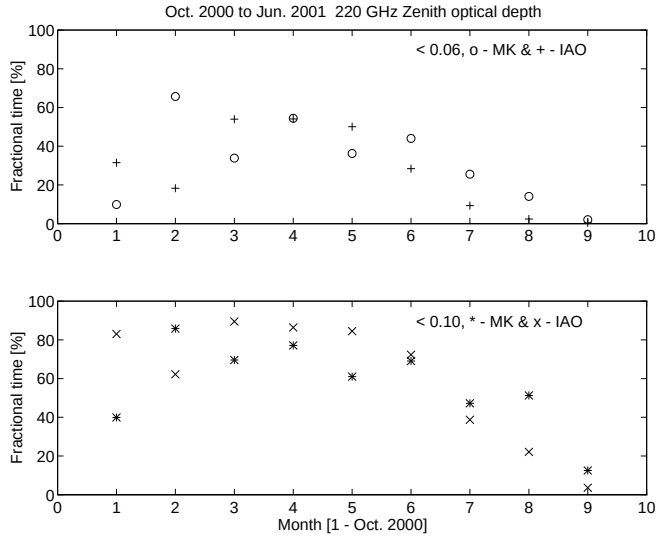

Figure 11. Fractional time at Mauna Kea and Hanle for 220 GHz opacity below 0.06 and 0.10. The Mauna Kea data is corrected to be equivalent to 220 GHz opacity by appropriately scaling it.

on the average for five winter months during 1994–95. The numbers for opacities below 0.06 for Atacama and the South Pole are about 60% and 85% respectively, which are better than for Hanle in 2001–02. All the numbers mentioned here are normalised to 220 GHz opacities, as the reported measurements were carried out at 225 GHz at Mauna Kea, Atacama and the South Pole.

Diurnal variations of opacity are also of interest in order to estimate the longest stretches of duration over which observations can be undertaken. Fig. 12 shows a plot of hourly variation of opacity on 20 December 2000. The change of opacity is rather slow and does not show a clear diurnal pattern. Thus it should be possible to observe continuously (day and night) from Hanle in the mm and sub-mm wavelength bands.

Conclusions

It is evident from the data presented in this paper, that Hanle has considerable advantage for observations in mm and sub-mm region. The results presented here indicate a positive offset between measured and

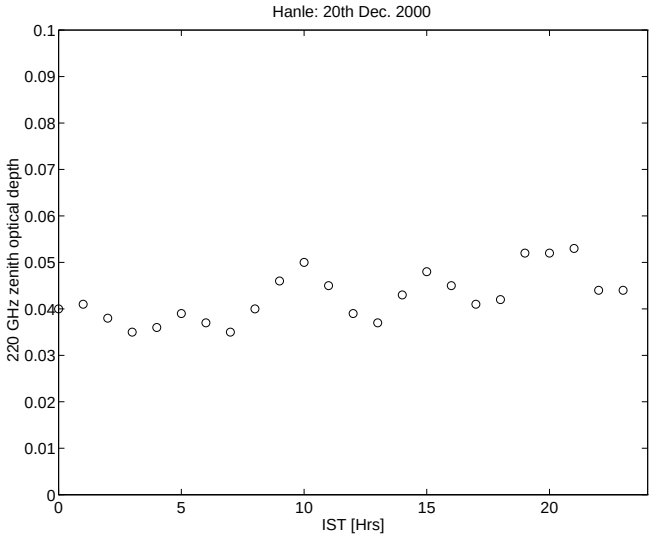

Figure 12. Typical diurnal zenith opacity (averaged hourly) for one of the best days.

expected opacities which need to be resolved in future investigations. One needs to reduce the systematic errors in the radiometer itself, and also to cross-calibrate the weather station data to see if the initial calibration has drifted. It will also be useful to launch a few radiosonde balloons at the site to estimate the detailed structure of water vapour distribution and its scale height.

Mt. Saraswati peak is in the middle of Nilamkhul plain (4250 m altitude) through which the Hanle river and a few underground streams meander. Though the amount of water flowing through is small and not turbulent, there is a possibility that these water sources add to the local water vapour in the summer months. There are other peaks to the northeast which are possibly less affected. A well established correlation between 220 GHz zenith optical depth and *pwv* derived from surface relative humidity and air temperature measurements will help in identifying drier sites, by just setting up another weather station.

We conclude that we have found and evaluated quantitatively a new site for sub-mm astronomy in the northern hemisphere. Higher and drier sites are available in the vicinity of Hanle for further characterisation.

Acknowledgements

A collaborative programme with remote operation of this kind could not be carried out successfully without active contributions from many. The actual list is quite long to be fully mentioned here. We express our appreciation of help from the following colleagues. T. Ito (UoT) for system integration and initial tests at UoT during Feb. 1999; B.R. Madhava Rao, R.R. Reddy (IIA) for fabrication and erection of pedestal and installation of radiometer; Angchuk Dorje, Mohinder Pal Singh and Tsewang Punchok (IIA) for system installation, data retrieval and continuous up-keep over nearly two years; K.B. Raghavendra Rao (RRI) for system integration and testing at RRI, before the system was transported to the Hanle site; T.K. Sridharan (CFA) for pointing out the expected low median opacities by reducing the weather data, comparing other sites; N. Kumar, D.K. Ravindra (RRI) and R. Cowsik (IIA) for continued support and encouragement. PGA thanks V. Radhakrishnan, N.V.G. Sarma (RRI) , Rajaram Nityananda (NCRA), T.K. Sridharan for very useful discussions and A.A. Deshpande for critical reading of the manuscript. We thank Richard A. Chamberlin of CSO for readily supporting the comparison with current 225 GHz opacity data at Mauna Kea.

References

1. HIROT Team 1996, Bull. astr. Soc. India, 24 p. 859.
2. Anupama G. C. 2000, Bull. Astr. Soc. India, 28, p. 647.
3. Cowsik, R., Srinivasan R., & Prabhu, T. P. (in press), In Proc. Workshop SITE 2000, ASP Conf. Ser.
4. Radford, S. J. E., & Chamberlin, R. A, 2000, ALMA Memo No. 334.1.
5. Matsushita, S., Matsuo, H., Pardo, J. R., & Radford, S. J. E., 1999, PASJ, 51, p. 603.
6. Hirota, T., Yamamoto, S., Sekimoto, Y., Kohno, K., Nakai, N., & Kawabe, R., 1998, PASJ, 50, p. 155.
7. Matsuo, H., Sakamoto, A., & Matsushita S., 1998, PASJ, 50 p. 359.
8. Chamberlin, R. A., Lane, P. A., & Stark, A. A., 1997, ApJ, 476, p. 428.
9. Holdaway, M. A., Ishiguro, M., Foster, S. M., Kawabe, R., Kohno, K., Owen, F.N., Radford, S. J. E., & Saito, M., 1996, MMA Memo No. 152.
10. Sekimoto, Y., Yoshida, H., Hirota, T., Takano, Y., Furuyama, E., Yamamoto, S., Saito, S., Ozeki, H., Inatani, J., Ohishi, M., Cardiasmenos, A. G., & Hensel, S. L., 1996, Intl. J. IR & MM Waves, 17, p. 1263.
11. Butler, B., 1998, MMA Memo No. 238.
12. Liebe, H. J., 1989, Int. J. IR & MM Waves, 10, p. 631.
13. Guillermo, D., Otarola, A., Belitsky, V., Urbain, D., Hills, R., & Martin-Cocher, P., 1999, ALMA Memo No. 271.1.